*Proc. Natl. Acad. Sci. USA*
Vol. 94, pp. 4745–4750, April 1997
Neurobiology

# Repair of plasmalemmal lesions by vesicles

**(crayfish medial giant axon/axotomy)**

CHRISTOPHER S. EDDLEMAN*, MARTIS L. BALLINGER†, MARK E. SMYERS†, CHRISTOPHER M. GODELL*†, HARVEY M. FISHMAN*, AND GEORGE D. BITTNER*†‡

*Department of Physiology and Biophysics, University of Texas Medical Branch, 301 University Boulevard, Galveston, TX 77555-0641; and †Department of Zoology, College of Pharmacy and Institute for Neuroscience, University of Texas, Austin, TX 78712

*Communicated by Donald Kennedy, Stanford University, Stanford, CA, February 28, 1997 (received for review May 9, 1996)*

**ABSTRACT** **Crayfish medial giant axons (MGAs) transected in physiological saline form vesicles which interact with each other, pre-existing vesicles, and/or with the plasmalemma to form an electrical and a physical barrier that seals a cut axonal end within 60 min. The formation of this barrier (seal) was assessed by measuring the decay of injury current at the cut end; its location at the cut end was determined by the exclusion of fluorescent hydrophilic dye at the cut end. When a membrane-incorporating styryl dye was placed in the bath prior to axonal transection and a hydrophilic dye was placed in the bath just after axonal transection, many vesicles near the barrier at the cut axonal end had their limiting membrane labeled with the styryl dye and their contents labeled with the hydrophilic dye, indicating that these vesicles originated from the axolemma by endocytosis. This barrier does not form in $Ca^{2+}$-free salines. Similar collections of vesicles have been observed at regions of plasmalemmal damage in many cell types. From these and other data, we propose that plasmalemmal lesions in most eukaryotic cells (including axons) are repaired by vesicles, at least some of which arise by endocytosis induced by $Ca^{2+}$ inflow resulting from the plasmalemmal damage. We describe several models by which vesicles could interact with each other and/or with intact or damaged regions of the plasmalemma to repair small (1–30 $\mu$m) plasmalemmal holes or a complete transection of the plasmalemma.**

To survive plasmalemmal damage, a cell must rapidly form a barrier which prevents the gain of deleterious substances (e.g., $Ca^{2+}$) and the loss of essential substances (e.g., proteins). Such a barrier (seal) must consist of a nonconducting lipid layer (i.e., membranous material) that is continuous except for submicroscopic (<10 nm) pores or channels. The repair of plasmalemmal damage has not been well studied. Repair of transected axons has usually been assumed to occur by a complete collapse and fusion of the axolemmal leaflets at the cut end (1–5) or by the formation of a single, continuous membranous partition at the cut end (6). In contrast, we recently showed that the sealing of transected myelinated earthworm medial giant axons (MGAs) was associated with the aggregation of vesicles at incompletely closed cut ends (7). However, we had no direct evidence whether this accumulation of vesicles and/or myelin delaminations created a diffusion barrier and where such a barrier might be located with respect to the vesicular aggregation. Furthermore, we did not know the origin of any of the vesicles, whether such vesicles collected at regions of lesser axolemmal damage (e.g., 1- to 30-$\mu$m holes), or whether vesicles collected at sites of plasmalemmal damage in other axons or in other cell types of other phyla.

We now report that crayfish MGAs (unmyelinated) transected in physiological salines containing $Ca^{2+}$ form vesicular aggregations at incompletely closed cut ends. These vesicles and other membranous structures constitute a barrier to the diffusion of hydrophilic dye. The formation of this dye diffusion barrier is correlated with the formation of a barrier to ionic movement as measured by the decay of injury-current density ($I_i$) at 60 min posttransection to values equivalent to control-current densities ($I_c$) measured for the intact axon prior to its transection. We have observed that vesicles which arise by endocytosis collect at cut ends or at small holes in unmyelinated or myelinated axons from various phyla (molluscs, annelids, arthropods, vertebrates). Given these data and data from other publications or observations, we describe several models for the repair of various plasmalemmal lesions by vesicles that interact with each other and/or the plasmalemma.

## MATERIALS AND METHODS

MGAs were dissected from crayfish (*Procambaris clarkii*) ventral nerve cords in physiological saline: 205 mM NaCl, 5.4 mM KCl, 2.6 mM MgCl, 13.5 mM $CaCl_2$, and 10.0 mM Hepes (pH 7.4). Our $Ca^{2+}$-free saline omitted $CaCl_2$ and added 1 mM EGTA. Our divalent-cation-free saline consisted of 205 mM NaCl, 5.4 mM KCl, 10.0 mM Hepes, 24.15 mM tetraethylammonium, 1.0 mM EGTA, and 1.0 mM EDTA. MGAs were transected with microscissors or a microknife made from a shard of a double-edged razor blade.

To assess the extent of sealing electrophysiologically in transected crayfish MGAs, we extracellularly measured $I_i$ at the cut end using a vibrating probe (7–9) and intracellularly measured membrane potential ($V_m$) within 50–100 $\mu$m of the cut end (7). Prior to transection, $I_c$ was surveyed at various points along the entire length of the axon with the probe tip placed about 30 $\mu$m from the intact axolemma (7, 8). After transection, the probe tip was placed opposite a cut end at a location that gave a maximum value for $I_i$. If $I_i$ decayed to $I_c$, then either the axon had reestablished an electrical barrier equivalent to that in the intact axon prior to transection or the axon was exceedingly depolarized (7). If the axon had an $I_i$ less than 15 $\mu A/cm^2$ ($I_c$ ranged from 3 to 15 $\mu A/cm^2$) and had a normal $V_m$ near its cut end, then the axon was considered to be unequivocally sealed electrically. Using this procedure, we measured $I_i$ from 3 to 120 min after transection.

To assess sealing morphologically, we examined intact and severed MGAs *in vitro* with differential interference contract (DIC) optics and thick or thin sections of fixed MGAs with

The publication costs of this article were defrayed in part by page charge payment. This article must therefore be hereby marked "*advertisement*" in accordance with 18 U.S.C. §1734 solely to indicate this fact.


0027-8424/97/944745-6$2.00/0
PNAS is available online at **http://www.pnas.org**.

Abbreviations: DIC, differential interference contrast; $I_c$, control current density; $I_i$, injury current density; MGA, medial giant axon; $V_m$, membrane potential; FITC, fluorescein isothiocyanate.

‡To whom reprint requests should be addressed at: Department of Zoology, University of Texas, Austin, TX 78712-1064.

photomicroscopy or electron microscopy. We examined the ability of the cut ends of an MGA to exclude or take up bath-applied pyrene using fluorescence microscopy with a Zeiss ICM-35 and other hydrophilic dyes using confocal fluorescence imaging with a Zeiss LSM 410. Pyrene dye (excited at 390–440 nm) fluorescence is concentration dependent so that its color is a sensitive indicator of the uptake of pyrene by the cut end of MGAs viewed with a Zeiss ICM-35. We also examined the ability of an MGA to retain hydrophilic dyes in an internal saline (109 mM KF/37 mM KAcetate/15 mM NaCl/96 mM mannitol/5 mM Hepes) injected into the axoplasm prior to severance. No differences were noted in the ability of MGAs to take up, exclude, or retain different hydrophilic dyes when these dyes were added to the bath saline after axonal transection. Fluorescent lipid-incorporating styryl dye (10) placed in the bath was used to label the axolemma and glialemma. When styryl dyes were placed in the bath saline for 5–10 min and then washed out with dye-free saline, the plasmalemma of the axons and glia were fluorescently labeled and remained labeled for more than 1 h after the dye was washed out. Hydrophilic dyes [fluorescein isothiocyanate (FITC)–dextran (488 nm), Lucifer Yellow (488 nm), Oregon Green–dextran (488 nm), pyrene, Texas Red–dextran (568 nm), tetramethylrhodamine–dextran (l,568 nm)] and membrane-incorporating styryl dyes [FM1-43 (488 nm), FM4-64 (568 nm)] were obtained from Molecular Probes. To determine dye uptake on exclusion, we compared the fluorescence in a severed axon to its fluorescence level prior to transection and/or to a paired intact axon (see figure 2 of the accompanying paper, ref. 11).

## RESULTS AND DISCUSSION

$I_i$ measured at the cut end at 3–5 min after transection became very large (>50 times) compared with $I_c$ measured across the intact axolemma of the axon prior to its transection in physiological saline (Table 1). $V_m$ measured within 50–100 $\mu$m of the cut end of transected MGAs was significantly ($P < 0.05$, Student's $t$ test) depolarized compared with resting $V_m$ of intact MGAs (Table 1). At 60 min posttransection, $I_i$ and $V_m$ were not significantly ($P > 0.05$) different from $I_i$ or $V_m$ recorded from intact MGAs—i.e., the axon had sealed (7, 9). When $I_i$ and $V_m$ were measured for MGAs transected in divalent-cation-free saline (Table 1) at 5 or 60 min after transection, the $I_i$ vector was always very large, inward, and directed toward the opening at the cut end and $V_m$ was significantly ($P < 0.05$) depolarized compared with intact MGAs—i.e., the axon had not sealed (7, 9).

To confirm that a physical barrier to diffusion formed at the cut end within 60 min after transection, we severed MGAs in physiological saline and added 1% pyrene dye to the bath at 60 min posttransection. At 75 min posttransection, we washed off the dye and then imaged the MGA. Most MGAs did not fluoresce (Fig. 1*A*; Table 1)—i.e., most MGAs excluded dye—indicating that the cut ends had sealed. As one control, when pyrene dye was added to the bath ≤20 min after transecting an MGA ($n > 15$) in physiological saline, pyrene dye was often observed to diffuse into the cut end within 5–10 min after its addition. As a second control, when intact axons ($n > 10$) were placed in physiological saline containing pyrene for 20 min, the MGAs did not exhibit axoplasmic fluorescence. When $Ca^{2+}$-free or divalent-cation-free saline was substituted for physiological saline, significantly fewer ($P < 0.01$, $\chi^2$ test) transected MGAs excluded pyrene dye at their cut ends (Table 1; Fig. 1*B*).

To determine what structures were associated with the barrier to dye exclusion, we viewed MGAs ($n > 60$) using both DIC optics and confocal fluorescence imaging (Figs. 1 *C–G* and 2 *A–D*), as well as photomicrographs and electron micrographs (Fig. 3). Intact MGAs were surrounded by a glial sheath consisting of 2–3 layers of glial processes alternating with collagen layers (12). At higher magnifications, the cortical layer of axoplasm contained mitochondria, microtubules, vesicles (<2 $\mu$m), and profiles of smooth endoplasmic reticulum. Intact MGAs had very few vesicles ≥1 $\mu$m diameter (Figs. 1*E* and 3*A*) and excluded hydrophilic fluorescent dye placed in the bath (Fig. 1*E*). Within minutes after MGAs were transected in physiological salines, vesicles 1–20 $\mu$m in diameter appeared in subaxolemmal regions near the cut end. Shortly after transection, the cut end typically narrowed to a small fraction (3–20%) of its original diameter (80–150 $\mu$m), but never completely closed (5–20 $\mu$m opening). The glial sheath did not completely cover the cut end, but rather terminated at the pore-like opening (Fig. 3*B*). Many vesicles (some as large as 20–30 $\mu$m in diameter) accumulated at this opening (Figs. 1*F*, 2 *C* and *D*, and 3*B*); vesicles were also present in the cortical (subaxolemmal) region of severed MGAs for several hundred $\mu$m from the cut end (such vesicles were not present in the subaxolemmal regions of intact axons; Figs. 1*D* and 3*A*). The axolemma was completely absent or greatly disrupted for 100–200 $\mu$m proximal to this pore-like structure. Gliaplasm, containing rough endoplasmic reticulum and glial nuclei, was observed in the axoplasmic space (Fig. 3*B*) at regions where both the axolemma and glialemma were no longer continuous when viewed at higher magnifications.

When any one of several hydrophilic fluorescent dyes (see *Materials and Methods*) was added to the extracellular bath

Table 1. Comparison of $I_c$, $I_i$, $V_m$, and dye exclusion in intact and transected crayfish MGAs

| | Intact | | Posttransection sampling time | | | |
|---|---|---|---|---|---|---|
| | | | Physiological saline | | Divalent-cation-free saline | |
| | Physiological saline | Divalent-cation-free saline | 5 min | 60 min | 5 min | 60 min |
| Pretransection measure | | | | | | |
| $I_c$, $\mu A/cm^2$ | 8 ± 5 (5) | 10 ± 3 (4) | | | | |
| $V_m$, mV | −86 ± 2 (7) | −82 ± 7 (6) | | | | |
| Posttransection measure | | | | | | |
| $I_i$, $\mu A/cm^2$ | | | 661 ± 279* (8) | 10 ± 7 (8) | 521 ± 84* (3) | 93 ± 11* (3) |
| $V_m$, mV | | | −36 ± 8* (3) | −80 ± 5 (5) | −28 ± 5* (3) | −26 ± 17* (4) |
| Dye exclusion technique | | | | | | |
| Confocal fluorescence | | | NA | 35/37 | NA | 0/6* |
| Fluorescence | | | NA | 39/42 | NA | 2/14,* 9/43*† |

$I_c$, $I_j$, and $V_m$ are given as the average ± SEM for sample size ($n$). Dye exclusion is given as the number of MGAs excluding dye divided by the number of MGAs sampled. Dye exclusion is given for confocal fluorescence images of hydrophilic dyes (confocal fluorescence) and for fluorescence images of pyrene dye (fluorescence). NA, not applicable.
*Significantly ($P < 0.05$) different from control values.
†Dye exclusion in $Ca^{2+}$-free saline.

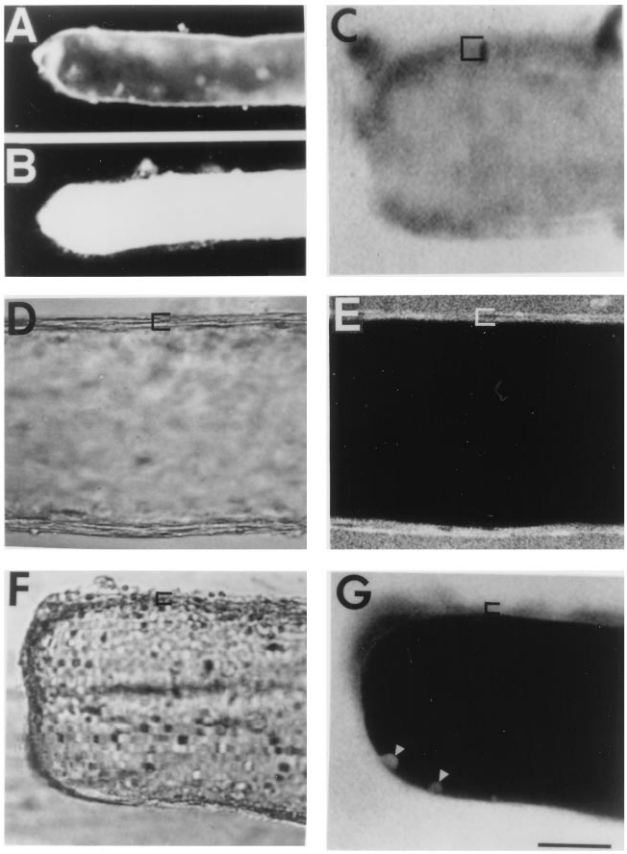


FIG. 1. Dye uptake/exclusion by MGAs. Cut end of transected axons are oriented to the left in all figures. In fluorescent images, black represents lack of fluorescence. In all confocal images using a Zeiss LSM 410, the <5-$\mu$m-thick confocal plane is parallel to, and through, the midsection of the long axis of an MGA. Brackets show the extent of glial sheath. (*A*) Sealed MGA in physiological saline. (*B*) Unsealed MGA in $Ca^{2+}$-free saline: fluorescence images where dye-free saline was replaced with 1% pyrene-saline at 60 min postseverance and replaced 15 min later with dye-free saline. (*C*) Confocal fluorescence image where dye-free, divalent-cation-free saline was replaced at 75 min postseverance with 0.1% FITC–dextran in divalent-cation-free saline for 15 min. [Compare fluorescing axoplasm in this unsealed axon with nonfluorescing axoplasm in confocal images of intact (*E*) or sealed (*G*) axons.] (*D* and *E*) DIC and confocal fluorescence images of intact MGA maintained in physiological saline for 60 min before adding 0.1% Texas Red–dextran for 45 min. (*F* and *G*) DIC and confocal fluorescence images of cut end of MGA where physiological saline was replaced at 75 min postseverance with 0.1% Texas Red–dextran for 15 min. Each line of all confocal images in this and the following paper was built up as the average of 8 line scans. Arrowheads indicate dye-filled vesicles or plasmalemmal invaginations. (Bar = 170 $\mu$m for *A* and *B*, 60 $\mu$m for *C–G*.)

<20 min after an MGA had been severed, the cut ends of these transected MGAs ($n = 5/5$) did not exclude dye in confocal fluorescence images. In contrast, when any one of these hydrophilic dyes (e.g., Texas Red–dextran) was added to the extracellular bath 60 min after an MGA had been severed, most (Table 1) MGAs did exclude the dye when imaged at 90 min posttransection (Figs. 1*G* and 2*A*). We determined the location of the dye barrier by placing one hydrophilic dye (e.g., FITC–dextran) intracellularly by injection prior to transection and another hydrophilic dye (e.g., Texas Red–dextran) extracellularly at 60 min posttransection. When the confocal fluorescence pattern for each dye was imaged at the cut end of such an MGA at 90 min posttransection, the boundary at which the intracellular dye was excluded from exiting the axon (Fig. 2 *B*) and the boundary at which the extracellular dye was excluded from entering the axon (Fig. 2*A*) were both very abrupt (no more than 1 $\mu$m wide) and located in about the same place at the cut end (Fig. 2 *A* and *B* superimposed upon Fig. 2*D*). Some of these MGAs with different hydrophilic dyes placed intracellularly and extracellularly were also examined after adding a membrane-incorporating styryl dye placed extracellularly to determine whether membranous structures were located at the dye barrier to these hydrophilic dyes. For example, for the MGA shown in Fig. 2 *A* and *B*, a styryl dye (FM1-43) was added to the physiological saline at 95 min postransection and the MGA was imaged at 120 min posttransection. At this time, the fluorescence of the more recently added FM dye was more intense and was easily distinguished from the fluorescence of the previously injected FITC–dextran that had been substantially photobleached. The membranes of many vesicles which had accumulated at the cut end of this MGA were FM-labeled (Fig. 2*C*), and the location of these vesicles coincided with the location of the barrier to the intracellularly and extracellularly placed hydrophilic dyes (Fig. 2 *A* and *B*). Similar data were obtained from other MGAs ($n = 4$) which received a comparable experimental paradigm.

Overlays of confocal fluorescence and DIC images (e.g., overlay of Fig. 2 *A* with *D* or Fig. 1 *G* and *F*) showed that most vesicles that accumulated at the cut end were not dye-filled when hydrophilic dye was added to the bath saline at 60 min after transection. Other data (Fig. 2 *F*) showed that when hydrophilic dye was injected into the axon prior to transection, most of the vesicles that accumulated at the cut end were not dye-filled. Using time-lapse confocal microscopy, we observed that dye-filled vesicles which formed after transection migrated toward the cut ends of transected MGAs (data not shown). After the plasmalemma of an MGA was labeled by adding FM styryl dye to the bath for 5–10 min and then removing it prior to MGA transection, the membranes of many vesicles that accumulated at the cut end were dye-labeled when observed for up to 60 min after transection (Fig. 2 *G* and *H*). These observations suggest that many vesicles which accumulate at the cut end arise by endocytosis of the axolemma shortly after transection of an MGA. Dye-labeled vesicles of endocytotic origin were often observed to fuse when observed with time-lapse confocal microscopy (Fig. 2 *G* and *H*).

When crayfish MGAs were transected and maintained in divalent-cation-free saline for 60 min before adding hydrophilic dye to the bath, significantly fewer ($P < 0.01$, $\chi^2$ test) axons excluded dye when observed with DIC and confocal fluorescence microscopy (compare Fig. 1 *C* and *G*). Compared with intact MGAs ($n > 20$; Fig. 3*A*) or to MGAs transected in physiological salines ($n > 10$; Fig. 3*B*), vesiculation was substantially reduced in the first 5–15 min in MGAs transected in $Ca^{2+}$-free salines. At 60 min posttransection in $Ca^{2+}$-free salines, one MGA lacked pore-like constrictions (Fig. 3 *C*); five other MGAs did exhibit pore-like constrictions and some vesicles at the cut end (data not shown). These data show that $Ca^{2+}$ is necessary for sealing and that the formation of a pore-like structure and/or the accumulation of vesicles at the cut end is not sufficient for sealing.

The repair of various types of plasmalemmal damage to axons other than the crayfish MGA or to other cell types in various phyla is also associated with the accumulation of vesicles or other membranous structures at the lesion site. (*i*) We and others observe $Ca^{2+}$-dependent, injury-induced vesicles appearing at the cut ends of other unmyelinated invertebrate axons [e.g., squid giant axons (9, 11, 13, 14)]. (*ii*) Vesicles, multivesicular bodies, and myelin delaminations accumulate at the cut ends of myelinated invertebrate axons [earthworm MGAs (7)] and myelinated vertebrate axons [frog (15, 16) and rat sciatic axons (A. Sunio, M.L.B., and G.D.B., unpublished data)]. (*iii*) We have reported (see accompanying paper, ref. 11) that vesicles accumulate at the cut ends where a dye-diffusion barrier forms in squid giant axons transected in physiological salines containing a calcium-activated neutral

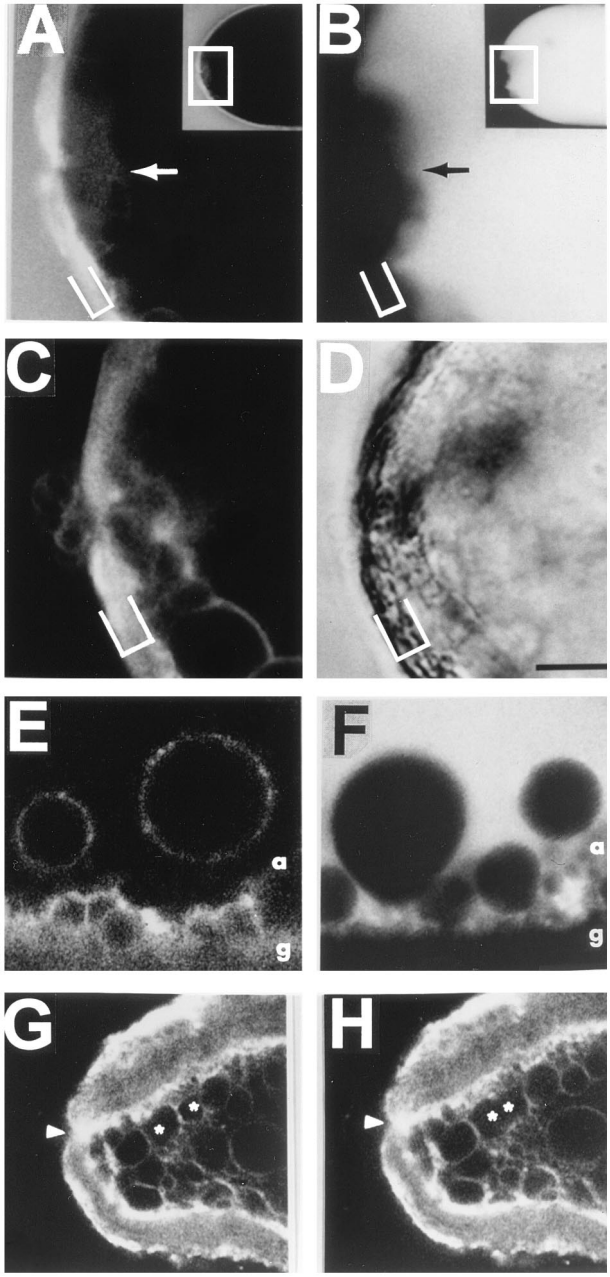


FIG. 2. Confocal fluorescence images of the cut end of an MGA transected in physiological saline with one hydrophilic dye placed extracellularly (*A*) and another placed intracellularly (*B*) showing the abrupt inner and outer dye boundaries at vesicular accumulations, vesicles labeled with a membrane-incorporating (10) styryl dye placed extracellularly (*C*) and the DIC image (*D*). Brackets mark limits of glial sheath. (*A* and *B*) Long-axis midsection fluorescence images both obtained at 90 min posttransection (*A*) Image of 0.1% Texas Red–dextran added to physiological saline 60 min posttransection. (*B*) Image of 0.1% FITC–dextran in intracellular saline injected into MGA prior to transection. Higher-magnification images correspond to the respective boxed areas in *Insets* (lower-magnification images). Arrow in *A* indicates location of outer dye barrier. Arrow in *B* indicates location of inner dye barrier. (*C*) Fluorescence image at 120 min posttransection of an MGA following addition of FM1-43 to the bath at 95 min posttransection. The fluorescence of the FITC–dextran was greatly reduced (photobleached) by prior illumination and was much less than the fluorescence intensity of the FM1-43 which was incorporated into the membranes of the vesicles at the cut end. (*D*) DIC image taken simultaneously with *C*. (*E* and *F*) Confocal fluorescence images in a transected MGA suggesting that vesicles arise from invaginations of the axolemma by endocytosis. a, Axoplasm; g, glial sheath. (*E*) Fluorescence image of an MGA after FM1-43 (25 $\mu$M) was added to the bath for 5 min and then removed from the bath prior to transecting the MGA. The membranes of many vesicles induced after transection were labeled with the styryl dye in a ring-shaped pattern when imaged in one confocal plane. (*F*) Fluorescence image of a transected MGA that was injected with 0.1% FITC–dextran in an internal saline solution prior to its transection. When imaged after transection, vesicles which formed after transection did not contain the hydrophilic dye. (*G* and *H*) Long-axis confocal fluorescence images taken from a series of time-lapse images of the cut end of an MGA pulse labeled with FM1-43 (25 $\mu$M) prior to transection showing a single fusion event of two vesicles, each marked by an asterisk. (*G*) Prior to fusion. (*H*) After fusion. Arrowhead marks the small pore at the cut end. (Bar in *D* = 20 $\mu$m for *A–D*, 85 $\mu$m for *Insets* in *A* and *B*, 5 $\mu$m for *E* and *F*, and 40 $\mu$m for *G* and *H*.)

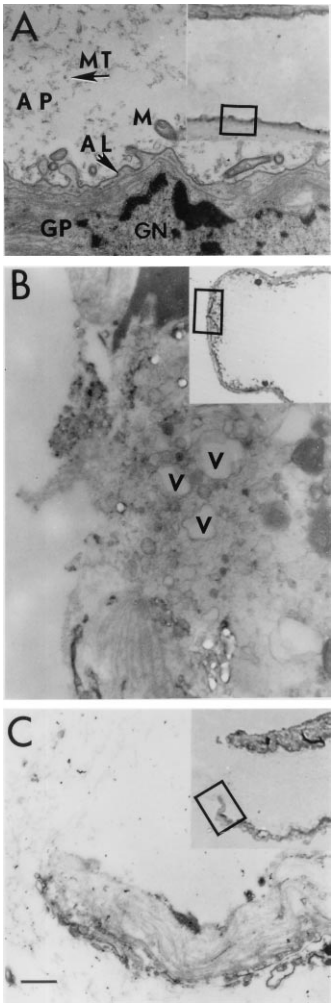


FIG. 3. Electron micrographs or photomicrographs (*Insets*) of longitudinal sections of intact MGAs in physiological saline (*A*) or severed in physiological saline (*B*) or severed in $Ca^{2+}$-free saline with 1 mM EGTA (*C*) and fixed 60 min later. AP, MGA axoplasm; MT, microtubules; M, mitochondria; AL, axolemma; GP, adaxonal layer of gliaplasm; GN, glial nucleus; (boxed area of *Inset* in *A*, glial layers; boxed area of inset in *B*, small pore at cut end; V, remnants of larger vesicles ($\geq$2 $\mu$m) often observed to burst when MGAs severed in physiological saline were exposed to fixative and imaged with DIC. (Bar = 1 $\mu$m for *A* and *C*; 0.5 $\mu$m for *B*; and 20 $\mu$m for *Insets A–C*.)

protease (calpain). (*iv*) We have observed (C.S.E., M.L.B., M.E.S., H.M.F., and G.DB., unpublished observations) that vesicles accumulate at the lesion site when 1- to 30-$\mu$m holes are made with a micropipette, a microscissors, or a focused laser beam in the axolemma of crayfish MGAs or squid giant axons in physiological salines. When observed with time-lapse confocal microscopy, vesicles rapidly appear by endocytosis in the subaxolemmal axoplasm and migrate from all directions to

the lesion site. Cessation of axoplasmic outflow from the lesion site is associated with the accumulation of vesicles at the lesion site within 20 min after lesioning and with the exclusion of hydrophilic dye placed in the bath saline. (*v*) A recent study (16) reports that masses of vesicles accumulate at regions of plasmalemmal disruptions in retinal endothelial cells and NIH 3T3 cells. We note that these vesicular masses resemble vesicular accumulations that we have observed at the cut ends of transected MGAs (Figs. 2 and 3) and other axons listed above. (*vi*) Small holes in unfertilized sea urchin eggs are repaired by $Ca^{2+}$-induced exocytosis of vesicles that exist in great numbers in the cortical cytoplasm just beneath the plasmalemma (17, 18).

Given all these data, we propose that most cells in eukaryotes repair various types of plasmalemmal damage by variants of an evolutionarily conserved process involving $Ca^{2+}$-induced vesiculation and interactions of vesicles with each other, the plasmalemma, and/or with other membranes. We further postulate that, while vesicles are always involved in the repair of various plasmalemmal lesions, the details of the repair process will almost certainly vary firstly with the type of lesion, secondly with the shape (morphological configuration) of the damaged cell membrane, and thirdly with the type of cell and its relationship to nearby cells.

Firstly, the type of lesion could be a small hole (ranging in size from less than a micrometer to tens of micrometers) in the plasmalemma or a complete transection of a cell. A small hole in eukaryotic cell membranes could be eliminated by vesicles in two ways: (*i*) direct repair by vesicular interactions with the boundary of the hole (Fig. 4*A1*) to form a toroidal structure (Fig. 4*A2*) which grows until the area circumscribed by the torus disappears as the torus is transformed into a sphere which then fills the hole and compresses due to surface tension (Fig. 4*A3*), or (*ii*) indirect repair (Fig. 4*B1*) by vesicular fusion with an intact portion of the plasmalemma (i.e., by exocytosis) near the hole (Fig. 4*B2*) so that the increase in lipid contributed to the plasmalemma by the fused vesicles produces closure of the hole (Fig. 4*B3*).

Secondly, the shape of a cell is also important with respect to the kind of repair mechanism that can be effective. A small hole or complete transection could occur in a spherically or nonspherically shaped cell. In cells that are spherical before injury or that become spherical after injury, the mechanisms described in Fig. 4 *A* and *B* could also repair a complete transection of a cell. However, these mechanisms, which assume that the addition of lipid/protein molecules to the plasmalemmal bilayer is not subjected to bending forces arising from disrupted or degraded cytoskeletal elements, by themselves cannot repair a completely transected nonspherical cellular projection—e.g., an axon, muscle fiber, or pseudopod from any cell type (Fig. 4*C1*). That is, vesicles (Fig. 4*C2*) which fuse with the remaining intact portion of a completely transected plasmalemma of a nonspherical cellular projection (Fig. 4*C3*) only extend the plasmalemma while the cut end remains open (Fig. 4*C4*). In contrast (Fig. 4*D1*), if vesicles (Fig. 4*D2*) move toward the cut end (Fig. 4*D3*), aggregate and interact (form junctional complexes) with each other and/or the plasmalemma to form a tightly packed plug (Fig. 4*D4*), then a barrier to diffusion (a seal) can be established at the cut end. Alternatively, vesicles might fuse with each other and with the plasmalemma (including large plasmalemmal invaginations) to form a continuous membrane barrier which seals off the cut end (Fig. 4*D5*).

Thirdly, the type of cell and its relationship to nearby cells determines the membranous sources from which vesicles are derived and the processes by which vesicles are formed. The origin of $Ca^{2+}$-induced vesicles probably depends on readily available sources. For example, in unfertilized oocytes, preformed vesicles (cortical granules) docked at the plasmalemma may repair small holes by $Ca^{2+}$-induced exocytosis (17, 18). However, most eukaryotic cells (including axons) do not have large numbers of vesicles predocked at the plasmalemma. Rather, in most eukaryotic cells, vesicles are induced upon elevation of intracellular $Ca^{2+}$ by inflow after injury (6, 7, 13, 15, 16, 19). In squid giant axons (12) and crayfish MGAs, $Ca^{2+}$-dependent endocytosis of axolemmal membrane induced after injury is a significant source of vesicular membrane (Fig. 2 *E* and *F*). This endocytosis may aid in sealing by shortening and constricting the cut end (20) by decreasing the surface area of the axolemma. This decrease in surface area may also generate a force that causes axoplasm and vesicles to flow toward the injury site. In squid and crayfish axons and

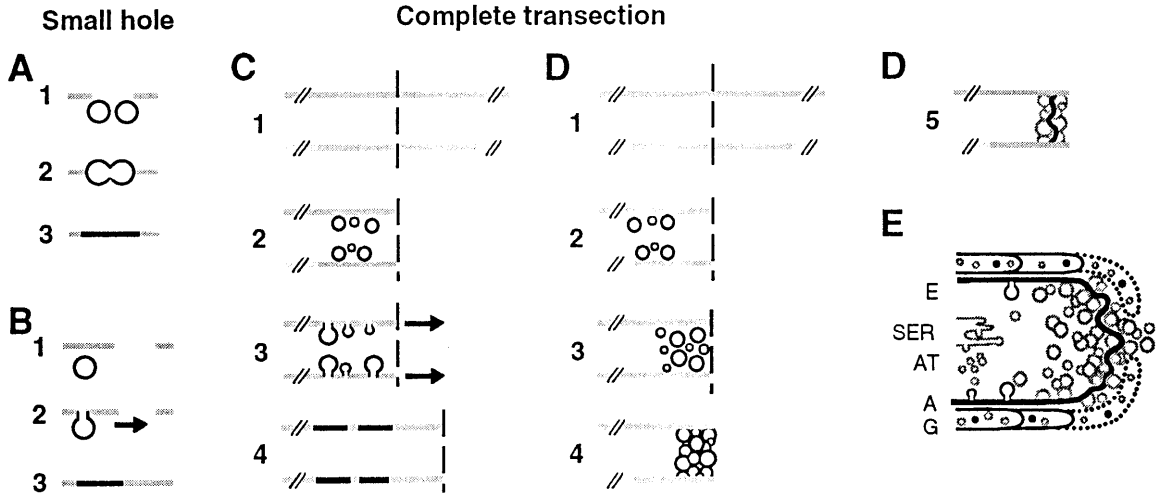


FIG. 4. Diagram showing mechanisms by which vesicles might seal a small hole (*A* and *B*) or a complete transection (*C* and *D*) of the plasmalemma in a nerve axon or any other eukaryotic cell. Small hole in plasmalemma represented by small break in line (*A2* and *B1*); complete transection represented by dashed line (*C1* and *D1*) which could be repaired by an aggregation of vesicles (*D4*) which may also help form a continuous membrane (represented by a darker solid line in *D5*). Schematic drawing (*E*) of a transected crayfish MGA in which vesicles that interact to help form a seal at the cut end may arise from endocytosis of the plasmalemma or glialemma (E), budding from the smooth endoplasmic reticulum (SER), axonal transport vesicles (AT), other glial membranes (G), etc. Dotted line represents disrupted glialemma or axolemma; solid line represents an intact, undamaged glialemma; heavy solid line (*A*) represents the axolemma which might be continuous with a newly formed continuous membrane at a cut axonal end. These membranes and/or interactions between vesicles that accumulate at the cut end form part of the seal at a cut end of a transected MGA. (See text for more details.)

most other cell types, injury-induced endocytosis of axolemma may also serve as a "seed" for fusion with other vesicular sources—e.g., vesicles involved in axoplasmic transport and vesicles derived from endoplasmic reticulum and other intracellular organelles. In axons, vesicles derived from glialemma, glial vesicles, or other glial membranous structures may also contribute membrane for seal formation. That is, we have observed on electron micrographs, in agreement with a previous report (7), that the glialemma and axolemma exhibit endocytosis, large invaginations and evaginations, and extensive disintegration for many micrometers near a cut axonal end—resulting in a mixing of axonal and glial membranous structures at the cut ends of squid, crayfish, and earthworm axons. In earthworm MGAs, myelin delaminations, evaginations, and other membranous structures from glia adjacent to the injury site also contribute significantly to vesicle formation and/or to other membranes that accumulate at the cut ends (7). This multi-source origin of membrane postulated for injury-induced vesicles is in agreement with the presence of nonaxolemmal ion channels in patch clamps of injury-induced vesicles extruded from transected squid giant axons (13). In fact, cells probably use whatever membrane sources are at their disposal, recycling and/or redistributing endogenous membrane or exogenous membrane from adjacent supporting cells to produce vesicles that repair damage to the plasmalemma.

Finally, since various data (Table 1, Figs. 1–3, and refs. 6, 7, and 17) show that the formation of a plasmalemmal seal requires $Ca^{2+}$, we now propose that $Ca^{2+}$ entry at sites of plasmalemmal damage has a dual role: (*i*) $Ca^{2+}$ entry activates $Ca^{2+}$-dependent pathways that degrade cytoskeletal and other proteins (21–24) and lead to cell death (25), and (*ii*) $Ca^{2+}$ entry initiates or facilitates $Ca^{2+}$-dependent processes necessary for the rapid repair of plasmalemmal damage. The following paper examines how the activation of a $Ca^{2+}$-dependent enzyme (calpain) promotes the sealing of transected squid GAs and crayfish MGAs.

We thank Mr. Alan Shipley, Mr. Louis Kerr, and Mr. Lee DeForke, Jr. for technical assistance and Dr. Yuri Magarshak for discussions of plasmalemmal repair mechanisms. We thank Dr. Claire Hulsebosch, Dr. Todd Krause, Dr. Sandra Tanner, and Dr. Guy Thompson for their comments on drafts of this manuscript, and David Bobb, Habacuc Garcia, and Abraham Thomas for assistance with confocal data. We thank Carl Zeiss Inc., and the Central Microscope and the National Vibrating Probe Facilities at the Marine Biological Laboratory (Woods Hole, MA) for use of their equipment. This work was supported by National Institutes of Health Grant NS31256 and an Advanced Technology Project grant.

1. Kao, C. C., Chang, L. W. & Bloodworth, J. M. B. (1977) *J. Neuropathol. Exp. Neurol.* **36,** 140–156.
2. Gallant, P. E. (1988) *J. Neurosci.* **8,** 1479–1484.
3. Xie, X. & Barrett, J. N. (1991) *J. Neurosci.* **11,** 3257–3267.
4. Kandel, E. R., Schwartz, J. H. & Jessell, T. M. (1992) *Principles of Neural Science* (Elsevier, New York), 3rd Ed.
5. Spira, M. E., Banbassat, D. & Dorman, A. (1993) *J. Neurobiol.* **24,** 300–316.
6. Yawo, H. & Kuno, M. (1983) *Science* **222,** 1351–1353.
7. Krause, T. L., Fishman, H. M., Ballinger, M. L. & Bittner, G. D. (1994) *J. Neurosci.* **14,** 6638–6651.
8. Jaffe, L. F. & Nuccitelli, R. (1974) *J. Cell Biol.* **63,** 614–628.
9. Krause, T. L., Magarshak, Y., Fishman, H. M. & Bittner, G. D. (1995) *Biophys. J.* **68,** 795–799.
10. Betz, W. J., Mao, F. & Bewick, G. S. (1992) *J. Neurosci.* **12,** 363–375.
11. Godell, C. M., Smyers, M. E., Eddleman. C. E., Ballinger, M. L., Fishman, H. M. & Bittner, G. D. (1997) *Proc. Natl. Acad. Sci. USA* **94,** 4765–4770.
12. Viancour, T. A., Seshan, K. R., Bittner, G. D. & Sheller, R. A. (1987) *J. Neurocytol.* **16,** 557–566.
13. Fishman, H. M., Tewari, K. P. & Stein, P. G. (1990) *Biochim. Biophys. Acta* **1023,** 421–435.
14. Gallant, P., Hammer, K. & Reese, T. S. (1995) *J. Neurocytol.* **24,** 943–954.
15. Lubinska, L. (1956) *Exp. Cell Res.* **10,** 40–47.
16. Miyake, K. & McNeil, P. (1995) *J. Cell Biol.* **131,** 1737–1745.
17. Steinhardt, R. A., Bi, G. & Alderton, J. M. (1994) *Science* **263,** 390–393.
18. Bi, G., Alderton, J. M. & Steinhardt, R. A. (1995) *J. Cell Biol.* **131,** 1747–1758.
19. Fishman, H. M. & Metuzals, J. (1993) *Biol. Bull.* **185,** 292–293.
20. Todora, M. A., Fishman, H. M., Krause, T. L. & Bittner, G. D. (1994) *Neurosci. Lett.* **179,** 57–59.
21. Schlaepfer, W. W. (1984) *Exp. Cell Res.* **67,** 73–80.
22. Pant, H. C. (1988) *Biochem. J.* **256,** 665–668.
23. Raabe, T. D., Nguyen, T. & Bittner, G. D. (1995) *J. Neurobiol.* **26,** 253–261.
24. Zimmerman, U. J. & Schlaepfer, W. W. (1984) *Prog. Neurobiol.* **23,** 63–78.
25. Trump, B., Berezesky, I., K. & Osorine-Vargas, A. R. (1981) *Cell Death in Biology and Pathology* (Chapman & Hall, New York), pp. 209–242.